KNMI-publication; 196-III

KNMI

Rainfall generator for the Meuse basin

Development of a multi-site extension for the entire drainage area

R. Leander, T.A. Buishand

Koninklijk Nederlands Meteorologisch Instituut

De Bilt, 2004

KNMI-publication; 196-III

De Bilt, 2004

PO Box 201, 3730 AE De Bilt
The Netherlands
Wilhelminalaan 10
http://www.knmi.nl
Telephone 030-22 06 911
Telefax 030-22 10 407

Author(s): R. Leander, T.A. Buishand

UDC: 551.506.2
551.577.2/.3
(282.244.11)
ISBN: 90-369-2265-8

● ● ● ●

Rainfall generator for the Meuse basin

Development of a multi-site extension for the entire drainage area

R. Leander, T.A. Buishand

KNMI-publication; 196-III

Work performed under contracts RI-2726 and RI-3414B to Ministry of Transport, Public Works and Water Management, Institute for Inland Water Management and Waste Water Treatment RIZA, P.O. Box 17, 8200 AA Lelystad (The Netherlands).
Telephone + 31.320.298411; Telefax +31.320.294218

Summary : A stochastic weather generator is constructed to simulate long series of precipitation and temperature for the Belgian and French Meuse basin. This weather generator is based on the principle of nearest-neighbour resampling, a method which samples daily data from a historic record with replacement such that the temporal and spatial correlations are preserved. The weather generator uses station records of temperature and precipitation as base material. A modification of the method is tested to simulate sub-catchment precipitation, for which only short records are available. To this end the weather generator is conditioned on a limited number of long station records. The standard deviations and autocorrelation coefficients of the simulated sub-catchment precipitation and the station temperatures are in good agreement with the estimates from the historical data. The distributions of the 4-, 10- and 30-day seasonal maxima of area-average precipitation are also well reproduced, although a rare historical 30-day event was found in July 1980, which was not exceeded in the 3000-year simulation.

---

1 Introduction

The Rhine and the Meuse are the most important rivers in the Netherlands. A large part of the country is situated in their delta. Protection against flooding is a point of continuous concern. Dikes and other flood protection works in the non-tidal part of the rivers have to withstand a discharge that is exceeded, on average, once in 1250 years (Middelkoop and van Haselen, 1999). Traditionally this design discharge is obtained from a statistical analysis of peak discharges (records starting from 1901 for the Rhine and from 1911 for the Meuse). An extensive evaluation of the design discharge for the Rhine was done by the first Boertien Commission (Delft Hydraulics and EAC-RAND, 1993). The design discharge for the Meuse received much less attention. However, shortly after the commission had completed its work, a large Meuse flood occurred in the south of the Netherlands. The second Boertien Commission was then appointed to formulate prevention measures to reduce future impacts of floods. For this commission a much more detailed analysis of the extreme Meuse discharges was carried out than under its predecessor (Delft Hydraulics, 1994). In 1996 the Flood Protection Act was established. This act prescribes the evaluation of the safety situation every five years. The last evaluation in 2001 led to new values of the design discharge of both the Rhine and Meuse (van de Langemheen and Berger, 2001).

The estimation of the 1250-year discharge event from statistical information in a record of about 100 years involves a strong extrapolation, which is quite uncertain. Furthermore, the extrapolation does not take into account the physical properties of the river basin. Therefore, the first Boertien Commission proposed the development of a hydrological/hydraulic model for the river basin of interest. The Institute for Inland Water Management and Waste Water Treatment (RIZA) adopted this idea in a research plan for a new methodology to determine the design discharge (Bennekom and Parmet, 1998). Besides the hydrological/hydraulic model, the development of a stochastic rainfall generator was also planned in order to produce long-duration rainfall series, containing unprecedented extreme events. This new methodology not only provides peak discharges, but also the temporal patterns of these extreme events and thus may give a better insight into the profile of the design discharge. Moreover, the new methodology also offers prospects to assess the potential impacts of climate change and the effect of retention measures.

After a pilot study (Buishand and Brandsma, 1996), KNMI started in 1996 with the development of a stochastic rainfall generator for the Rhine basin. A nearest-neighbour resampling technique was used to generate multi-site daily precipitation and temperature series (Wójcik et al., 2000). For the catchment of the Ourthe, a tributary of the river Meuse, the simulation of daily rainfall and temperature was extended with a disaggregation step to obtain 6-hourly values (Wójcik and Buishand, 2001). In this report the simulation of daily values for the entire Meuse basin is considered.

The Meuse is the second largest river in the Netherlands. The river originates on the plateau of Langres in northeastern France at an altitude of 409 m. After passing through France and the Belgian Ardennes, it enters the Netherlands a few kilometers south of Maastricht. The catchment area upstream of Borgharen (the gauging site near Maastricht) is about 21 000 km^2, whereof approximately 11 000 km^2 in Belgium. A number of station records were available for the Meuse basin, which were longer than the areal rainfall records for

the various sub-catchments. The possibility to make use of the information from these long records for generating areal rainfall is explored.

The report is organised as follows. Chapter 2 describes the data used in this study. Chapter 3 explains the method of nearest-neighbour resampling. Chapter 4 discusses the modification of the resampling algorithm to generate areal precipitation using relatively short areal precipitation records in combination with long station records. In Chapter 5 the simulation results for the entire Meuse basin are presented. Finally, in Chapter 6 the conclusions are formulated.

2 Description of the data used in the simulations

2.1 Station records of daily precipitation

The nearest-neighbour resampling technique requires uninterupted long records of daily precipitation from stations in and around the Meuse catchment. Figure 2.1 shows the geographical locations of 14 stations with long homogeneous daily precipitation records. The homogeneity of the French and Belgian records is discussed in Leander and Buishand (2004a). The homogeneity of the daily precipitation record for Aachen (Germany) has been assessed in a similar way.

Two base periods were considered for the simulations, 1930-1998 and 1961-1998. The 14 stations in Figure 2.1 have complete records for the shorter period and 7 of them have complete records for the period 1930-1998 (excluding 1940). Table 2.1 lists the average precipitation totals for the winter half-year (October to March) and the summer half-year (April to September). For the 7 stations with complete records for the period 1930-1998 the average winter amount for that period is 3.5% lower than the average for the sub-period 1961-1998. For the summer, the difference between the two periods is negligible. The wettest stations in France and southern Belgium (Neufchâteau, Le Chesne and Chiny) have relatively large precipitation amounts in the winter half-year.

Table 2.1: Average winter and summer precipitation totals for stations used for the simulations, calculated for the periods 1930-1998 and 1961-1998.

	Station name	Altitude [meters]	Precipitation totals [mm] 1961-1998 winter	1961-1998 summer	1930-1998* winter	1930-1998* summer
France	St. Quentin	95	358	344	339	340
	Reims	94	290	316	-	-
	Nancy	212	374	378	358	370
	Vouziers	96	380	363	367	361
	Chaumont	317	474	432	457	435
	Châteauvillain	230	451	424	-	-
	Langres	467	455	423	-	-
	Neufchâteau	286	515	428	-	-
	Le Chesne	174	536	425	-	-
Belgium	Uccle (Brussels)	100	417	405	403	398
	Chiny	299	728	529	717	542
	Stavelot	298	572	520	-	-
	Rochefort	193	406	422	-	-
Germany	Aachen	202	388	423	378	427
	7-station average		446	410	431	410

*the year 1940 was excluded

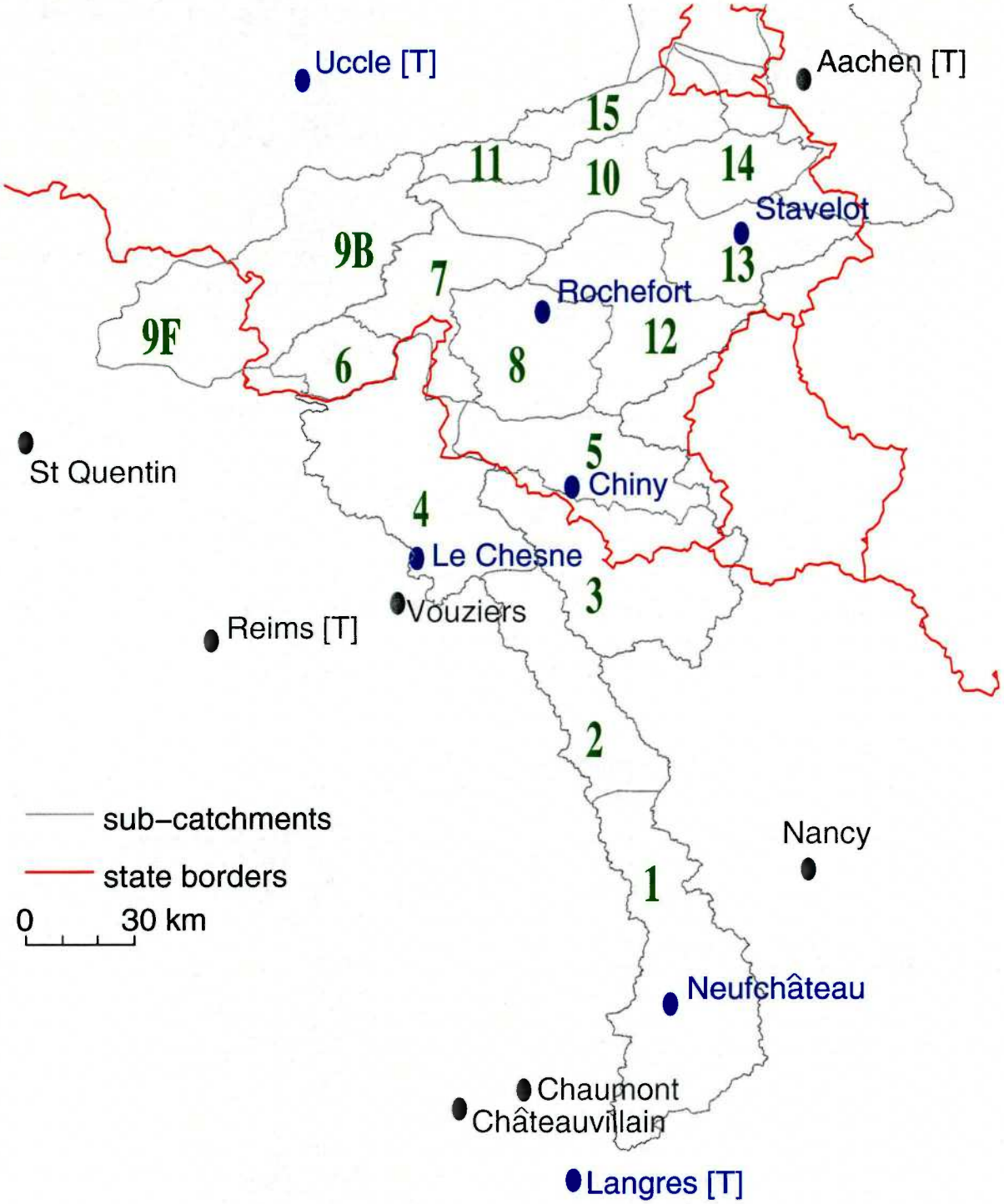

Figure 2.1: Locations of rainfall stations. The stations presented in blue form a subset used in the simulations based on the period 1961-1998. The grey contours and the green numerals show a subdivision of the Meuse basin into 16 sub-catchments. Stations providing a temperature record are marked with "[T]".

Table 2.2: List of French and Belgian sub-catchments of the Meuse. The mean area-average precipitation totals for the winter en the summer are given, based on the years 1961-1998.

			Precipitation totals [mm]	
	Sub-catchment	Area [km^2]	winter	summer
1	Meuse (St.Mihiel)	2575	487	425
2	Meuse (St.Mihiel-Stenay)	1283	497	412
3	Chiers	2192	500	415
4	Meuse (Stenay-Chooz)	2241	529	431
5	Semois	1213	695	506
6	Viroin	525	536	455
7	Meuse (Chooz-Namur)	1109	511	450
8	Lesse	1302	521	463
9B	Sambre (Belgium)	1679	445	419
9F	Sambre (France)	1055	445	408
10	Meuse (Namur-Liège)	1546	397	410
11	Mehaigne	344	396	404
12	Ourthe	1588	515	468
13	Amblève	1044	587	521
14	Vesdre	680	565	546
15	Jeker	455	388	416
	total area	20831	500	441

2.2 Catchment-average daily precipitation

The Meuse basin has been subdivided into 16 sub-catchments (Table 2.2), in correspondence with the subdivision used for hydrological modelling (van Deursen, 2004). The Sambre catchment was subdivided in a Belgian part 9B and a French part 9F. The area-average precipitation for the Belgian sub-catchments of the Meuse has been composed from records of area-average precipitation, obtained from the Royal Meteorological Institute of Belgium for the period 1951-1998. For the French sub-catchments areal precipitation was calculated from French station data using squared inverse distance interpolation on a grid (Leander and Buishand, 2004b). These records cover the years 1961 through 1998.

2.3 Station records of daily temperature

Four temperature records were used in this study: one Belgian record (Uccle), two French records (Langres and Reims) and one German record (Aachen), each marked with a "[T]" in Figure 2.1. Only the records from Uccle and Aachen are long enough to cover the period 1930 to 1998 completely. The average temperatures for the winter and summer half-year for these four stations are reported in Table 2.3, calculated over the period 1961-1998 and (if appropriate) the period 1930-1998, except 1940. The differences between the four stations are small, in particular in summer, demonstrating that the average temperature varies on a much larger spatial scale than the average precipitation.

The homogeneity of the temperature records has been roughly tested. The largest non-homogeneities ($\approx 0.5^oC$) were found in the records of Reims (around 1981) and Uccle (gradual trend). The records were not corrected for these non-homogeneities.

Table 2.3: Average winter and summer temperature for stations used for the simulations, calculated for the periods 1930-1998 and 1961-1998.

	Temperature [^{0}C]			
	1961-1998		1930-1998*	
Station	winter	summer	winter	summer
Reims	5.2	14.6	-	-
Langres	3.9	14.3	-	-
Uccle	5.6	14.8	5.5	15.0
Aachen	5.3	14.4	5.1	14.5

*the year 1940 was excluded

3 Nearest-neighbour resampling

3.1 Background

The concept of nearest-neighbour resampling was first presented by Young (1994) as a physically consistent method for simulating time series of several dependent weather variables. Independently, Lall and Sharma (1996) proposed a nearest-neighbour bootstrap to generate hydrological time series. In 1996 a first study was done by KNMI (Buishand and Brandsma, 1996), leading to a multi-site rainfall generator for the Rhine basin (Wójcik et al., 2000). The most important advantage of nearest-neighbour resampling compared to other stochastic weather generators is that it automatically preserves the correlation between multiple variables simulated simultaneously. Furthermore, due to the conditioning of new daily values on the preceding days, the autocorrelation of those variables can also be preserved, though there is a random element in the selection process. The reproduction of the autocorrelation of daily rainfall is in particular crucial for hydrological simulations for which the simulated precipitation serves as input, because large river flows are generally induced by persistent rainfall over a multi-day period. An important advantage of the method is that it requires no assumptions concerning statistical distributions and relationships, and that it is completely data-driven.

3.2 General principle of unconditional nearest-neighbour resampling

In nearest-neighbour resampling daily weather variables are sampled with replacement from the historical data to generate long daily sequences. It is required that these sequences have the same statistical characteristics as the historical data, such as the variability and temporal correlation. The multi-day totals in the generated sequences however can take values which are not observed in the historical sequence, due to the reordering of historical days. In each cycle of the algorithm the days in the historical record are sorted with respect to their similarity to the previously sampled day in terms of certain selected characteristics of the weather variables. One of the k closest days is selected at random and the weather variables of its historical successor are accepted as the data for the new day to be added to the sequence. This procedure is illustrated by Figure 3.1 for two variables. In earlier work for the Rhine basin this type of resampling is referred to as *unconditional*, as opposed to *conditional*, because the selection of the next day only depends on the previously sampled days.

In the resampling process each day, either in the generated sequence or the historical data, is characterised by a feature vector, which summarises precipitation and temperature at several locations. The extent to which two days t and u differ, is quantified by the weighted squared Euclidean distance $\delta^2(\mathbf{D}_u, \mathbf{D}_t)$ between their feature vectors $\mathbf{D}_u$ and $\mathbf{D}_t$, i.e.

$$\delta^2(\mathbf{D}_u, \mathbf{D}_t) = \sum_{j=1}^{p} w_j (D_{tj} - D_{uj})^2 \quad , \tag{3.1}$$

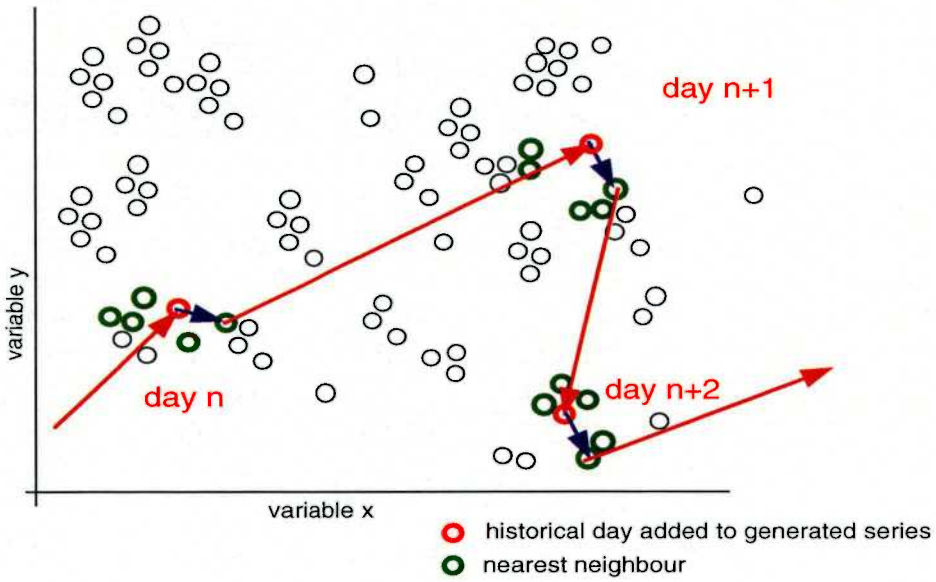

Figure 3.1: Schematic representation of the nearest-neighbour method for two variables. One of the $k = 5$ states (green) which are closest to that of the last sampled day (red) is selected at random (blue arrow), using a decreasing kernel. Its historical successor (red arrow) provides the values for the new simulated day.

where the index j refers to the jth of the p elements of the feature vectors. The corresponding weights w_j are determined for each of the feature vector elements as the inverse of their global sample variance (i.e. the mean squared deviation with respect to the total mean).

In the random selection of one of the k nearest neighbours, a decreasing kernel is used, which gives more weight to closer neighbours. The probability of selecting the jth closest neighbour is given by

$$p_j = \frac{1/j}{\sum_{i=1}^{k} 1/i} \,. \tag{3.2}$$

In this study $k = 10$ is used.

3.3 Standardisation of the data and composition of the feature vectors

The data used in the simulation were first standardised. This reduces the influence of the seasonal cycle on the selection procedure. The temperature T_t for historical day t is standardised with a smoothed temperature mean m_d and standard deviation s_d for the corresponding calendar day d using

$$\widetilde{T}_t = (T_t - m_d)/s_d. \tag{3.3}$$

Daily precipitation was standardised with an estimate $m_{d,wet}$ of the mean wet-day precipitation:

$$\widetilde{P}_t = P_t/m_{d,wet}. \tag{3.4}$$

In $m_{d,wet}$ only days with 0.3 mm of precipitation or more are taken into account. The estimates for the individual calendar days have been smoothed with the Nadaraya-Watson smoother using the Epanechnikov kernel (Wójcik et al., 2000) with a bandwidth of 45 days for $m_{d,wet}$ and a bandwidth of 30 days for m_d and s_d. Figure 3.2 displays m_d, s_d and $m_{d,wet}$ for the precipitation and temperature for the station Uccle.

The standardisation was carried out for the stations separately. In all simulations described in this study, the feature vector for day t consists of:

- The station-averaged standardised precipitation $\widetilde{P}_t$.
- The station-averaged standardised temperature $\widetilde{T}_t$.
- The total of average standardised precipitation for the preceding n_h days, i.e. $\widetilde{S}_t = \widetilde{P}_{t-1} + \widetilde{P}_{t-2} + \ldots + \widetilde{P}_{t-n_h}$ This element is included to enhance the persistence of the precipitation in the generated sequence, which is crucial in the reproduction of the variability of monthly amounts and extreme multi-day amounts. $\widetilde{S}_t$ is the only element of the last generated day that depends on the order in which days are sampled. Therefore, it needs to be recalculated for each new step. The value $n_h = 4$ was found to give optimal results and is used in the simulations shown here.

To further account for the seasonal variation in the data, the search for nearest neighbours was restricted to a 'window' of $W_{mw} = 61$ calendar days, centred on the last simulated day. This prevents that a summer day is preceded or succeeded by a typical winter day.

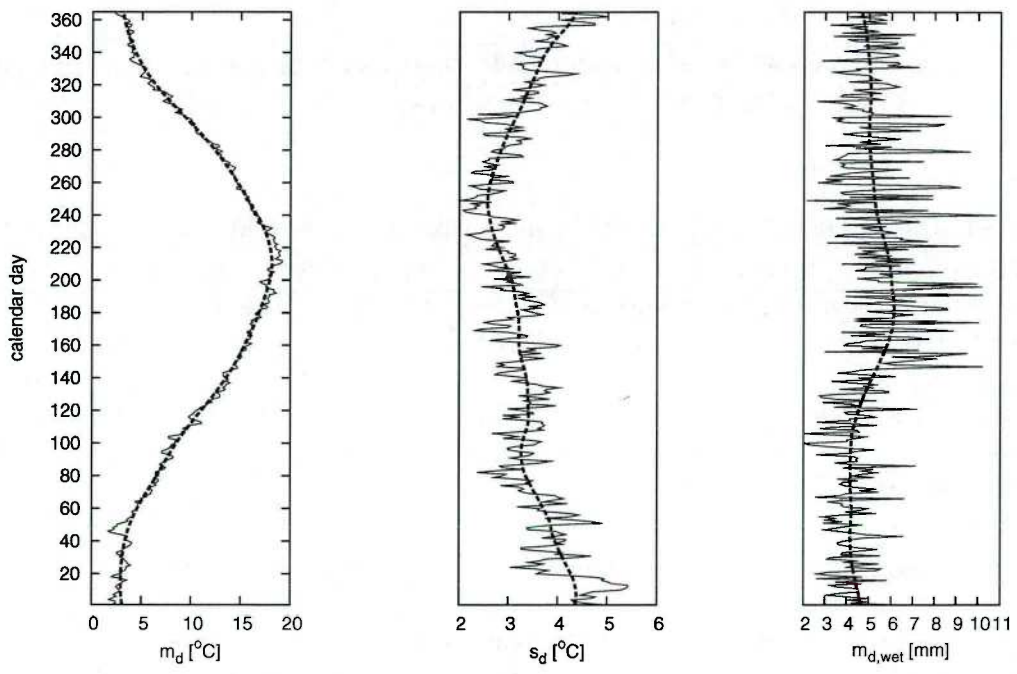

Figure 3.2: Values of m_d, s_d and $m_{d,wet}$ for the station Uccle for the period 1961-1998. The dashed curves represent the smoothed approximations.

3.4 The resampling algorithm

In summary, the concept of unconditional nearest-neighbour resampling can be outlined as follows:

1 Calculate the smoothed values of m_d, s_d and $m_{d,wet}$ for all calendar days and stations.

2 Standardise P and T data for each station separately, using m_d, s_d and $m_{d,wet}$.

3 Calculate summary statistics from standardised P and T series, composing a feature vector for each historical day in the considered base period.

4 Generate data for the first day ($t = 1$) by randomly sampling a day within the window for the 1st of January.

For each new simulated day {

5 Compose a feature vector $\mathbf{D}_t$ using standardised P and T data for the last simulated day t.

6 Find the k nearest neighbours of $\mathbf{D}_t$ within the window centred on day t.

7 Randomly select one of these nearest neighbours, using the decreasing kernel (3.2).

For each (standardised) weather variable {

8 Deliver the standardised precipitation and temperature data for the historical successor of the selected nearest neighbour as the standardised values for the new simulated day $t + 1$.

9 Transform the resampled standardised variables back to their original scale using the the reverse of (3.3) and (3.4).

}

}

Note that all stations are resampled simultaneously. Because the feature vector for day t contains the memory element $\widetilde{S}_t$, the first n_h historical days cannot be selected in the simulation, since their history is unknown. To determine $\widetilde{S}_t$ for the first n_h simulated days, the historical predecessors of the first selected day were used, as the values for $t = 0, -1, \ldots$.

In step 8 also variables can be delivered which are not contributing to the feature vectors, such as precipitation and temperature at nearby stations or areal precipitation. Such variables are referred to as 'passive' variables. These must also be standardised prior to the simulation. The generated sequences for these variables can however only be meaningful if they have some relation to the 'active' variables that comprise the feature vector.

In the next chapter the simulation of area-average precipitation for the Belgian sub-catchments as passive variables is explored. In addition, the algorithm is modified slightly to handle incomplete records.

4 Simulation of sub-catchment precipitation for the Belgian Meuse

4.1 Nearest-neighbour substitution of missing days

In order to make use of short or incomplete historical records of passive variables, the resampling algorithm in Section 3.4 is slightly altered. In the case that the historical values of passive variables required in step 8 are not available for the day of interest, an alternative day is selected from the available days in their record. The selection of this day is based on a nearest-neighbour search in terms of Euclidean distances between the feature vectors. In this case the feature vectors contain the station-average precipitation and temperature (from the same stations as in step 5), but *not* the memory element. Again a window of 61 calendar days is applied to limit the search for a nearest neighbour, but now it is centred on the calendar-day for which an alternative is sought.

The modified resampling algorithm was tested by simulating daily series of areal precipitation for the 11 Belgian sub-catchments in Figure 2.1 (numbered 5-8, 10-15 and 9B) as passive variables. The feature vector for these simulations was based on station records from Aachen, Chaumont, Uccle, Chiny, Nancy, Vouziers and St. Quentin for precipitation and Uccle and Aachen for temperature for the period 1951-1998. The areal rainfall data were available for the same 48-year period. In this chapter the effect of the modification on the statistical properties of the simulated series is investigated by leaving out certain segments of the records of areal precipitation for the sub-catchments.

4.2 Results

To investigate the influence of shortening the records of areal precipitation, five simulations were compared:

- using sub-catchment data for the full period of station data, denoted `51-98`
- using sub-catchment data only for the period 1975-1998, denoted `75-98`
- using sub-catchment data only for the period 1990-1998, denoted `87-98`
- using sub-catchment data only for the period 1951-1974, denoted `93-98`
- using sub-catchment data only for the period 1951-1974, denoted `96-98`.

Each simulation had a length of 1000 years. The statistical properties of the simulated areal precipitation have been compared to those of the historical series of sub-catchment precipitation for the period 1951-1998. Only the winter half-year was considered, which is the most relevant season for peak discharges of the Meuse. Table 4.1 summarises for all simulations the reproduction of the mean M and standard deviation s_M of the monthly amounts, the standard deviation s_D of the daily amounts and the first- and second-order autocorrelation coefficients r_1 and r_2. The jackknife method described by Buishand and Beersma (1993,1996), was used to obtain these statistics and their standard errors *se*. Differences between the historical and simulated values larger than twice the standard error of the estimate from the historical data are indicated as statistically significant. This

Table 4.1: Biases of the first- and second-order statistics for all five cases. The bias in the monthly mean $\overline{M}$ and standard deviation $\overline{s}_{M}$, the daily standard deviation $\overline{s}_{D}$ and the autocorrelation coefficients $\overline{r}_1$ and $\overline{r}_2$ for the winter half-year (October-March) are shown. The bottom lines give the estimates from the historical data and twice their standard error *se*. Significant biases are printed in bold.

	$\Delta\overline{M}$		$\Delta\overline{s}_{M}$		$\Delta\overline{s}_{D}$		$\Delta\overline{r}_1$	$\Delta\overline{r}_2$
51-98	-3.0	mm	0.4	%	0.5	%	-0.008	0.006
75-98	-4.1		-0.9		0.0		-0.021	-0.001
87-98	-3.7		-0.9		-0.4		-0.020	0.000
93-98	-5.0		-2.7		-1.3		**-0.029**	-0.003
96-98	**-11.8**		**-12.6**		**-12.2**		-0.015	0.008
Historical	82.5	mm	42.2	mm	4.4	mm	0.392	0.214
$2 \times se$	5.3	mm	8.4	%	5.0	%	0.028	0.022

roughly corresponds to a two-sided test at the 5% level. In order to make a fair comparison between the historical and the simulated series, the latter were split into 20 runs of 48 years (using the first 960 years of the simulation), which were assumed to be independent. All statistics in the table have been determined separately for each calendar month, sub-catchment and 48-year run and averaged over the six winter months and the 20 runs. Subsequently, (absolute or relative) differences from the historical values were calculated for each of the sub-catchments. Finally, an area-weighted average of these biases was calculated from the results for the sub-catchments. The calculation of the biases in the means, standard deviations and autocorrelation coefficients is explained in more detail in Section 5.1.

According to Table 4.1, the biases in the monthly mean and the monthly and daily standard deviation are only significant for simulation 96-98. For simulation 93-98 there is a significant bias in the first-order autocorrelation. The bias in the standard deviations is not significant for this simulation, but considerably larger than for the first three simulations in the table.

Figure 4.1 shows the autocorrelation function of basin-average precipitation for lags up to 9 days. The higher order autocorrelations are well reproduced. Except for the bias in the first-order autocorrelation coefficient of simulation 93-98, no significant bias is found in any of the other simulations. All simulations underestimate the first-order autocorrelation and overestimate the fourth and fifth-order autocorrelation. Clearly the reduction of the available amount of passive data and the substitution of missing days do not seriously affect the temporal correlation. It is further noted that the historical seventh-order autocorrelation coefficient is relatively high, which could indicate a weekly pattern in the data. This effect is not reproduced by the simulations.

Figure 4.2 displays the Gumbel plots of the winter maxima of 4-day and 10-day basin-average precipitation. Different simulation runs are shown for the case that the sub-catchment data for the period '51-'98 were used. These give an impression of the spread in the Gumbel plots inherent to a 1000-year simulation. Longer simulations will be required to reduce the spread. Considering the 4-day maxima, the difference between the original simulation 51-98 and simulation 75-98 is of the same order as the natural spread of different

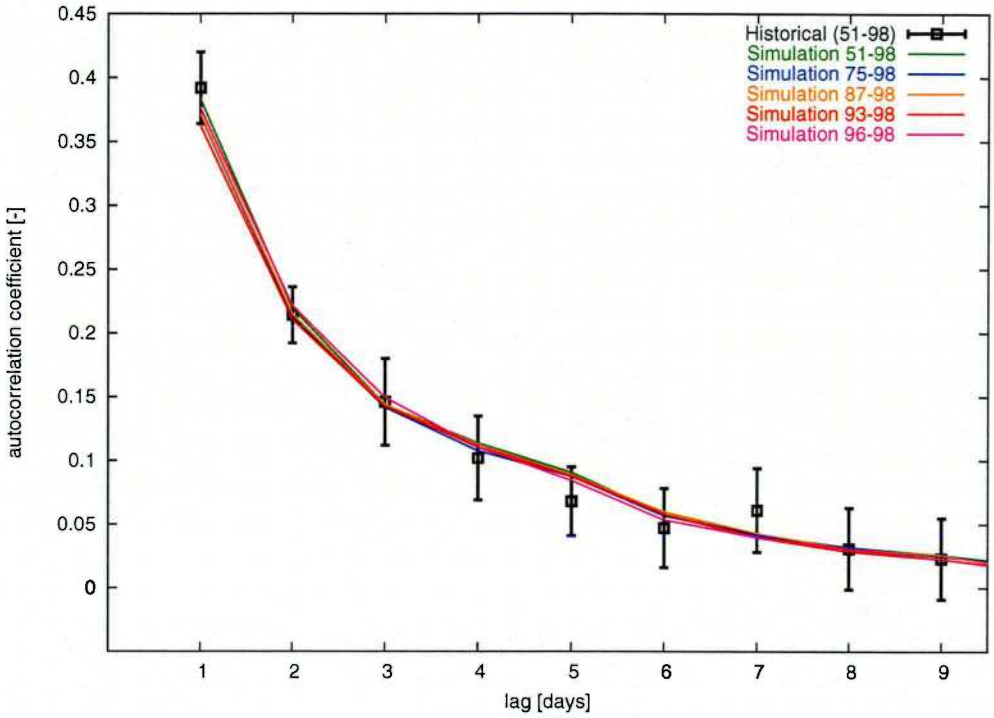

Figure 4.1: Autocorrelation coefficients of the five simulated series of daily basin-average precipitation and those obtained from the historical daily basin-average precipitation for the period 1951-1998. The latter are plotted with their $2 \times se$ intervals.

simulation runs using the same sub-catchment data. Both simulations show a good agreement with the historical data. The three highest historical values are somewhat below the simulated curves. The simulations 87-98 and 93-98 deviate more from simulation 51-98 than simulation 75-98, and these simulations slightly underestimate the intermediate historical quantiles with return periods roughly between 5 and 20 years. Simulation 96-98, finally, is clearly different from the other simulations. The curve passes straight through the highest historical value, but lies far below the rest of the plot for the historical data. For the 10-day maxima, on the other hand, the Gumbel plots of the different simulations (except simulation 96-98) are closer together and in good agreement with the plot for the historical maxima.

4.3 Conclusion

The results indicate that the statistical properties of indirectly simulated passive variables do not become worse when only a part of the records for these variables is used (except when the length of these records is reduced to three or six years). Second-order statistics and extremes of 4- and 10-day amounts are reproduced satisfactorily by most simulations. The autocorrelation remains unaffected by the substitution of missing values by an additional nearest-neighbour search, indicating that the persistence depends on the resampled feature vector series, rather than the individual daily values of the passive variable. This gives confidence that the modified resampling algorithm presented here indeed circumvents the problem of missing passive data.

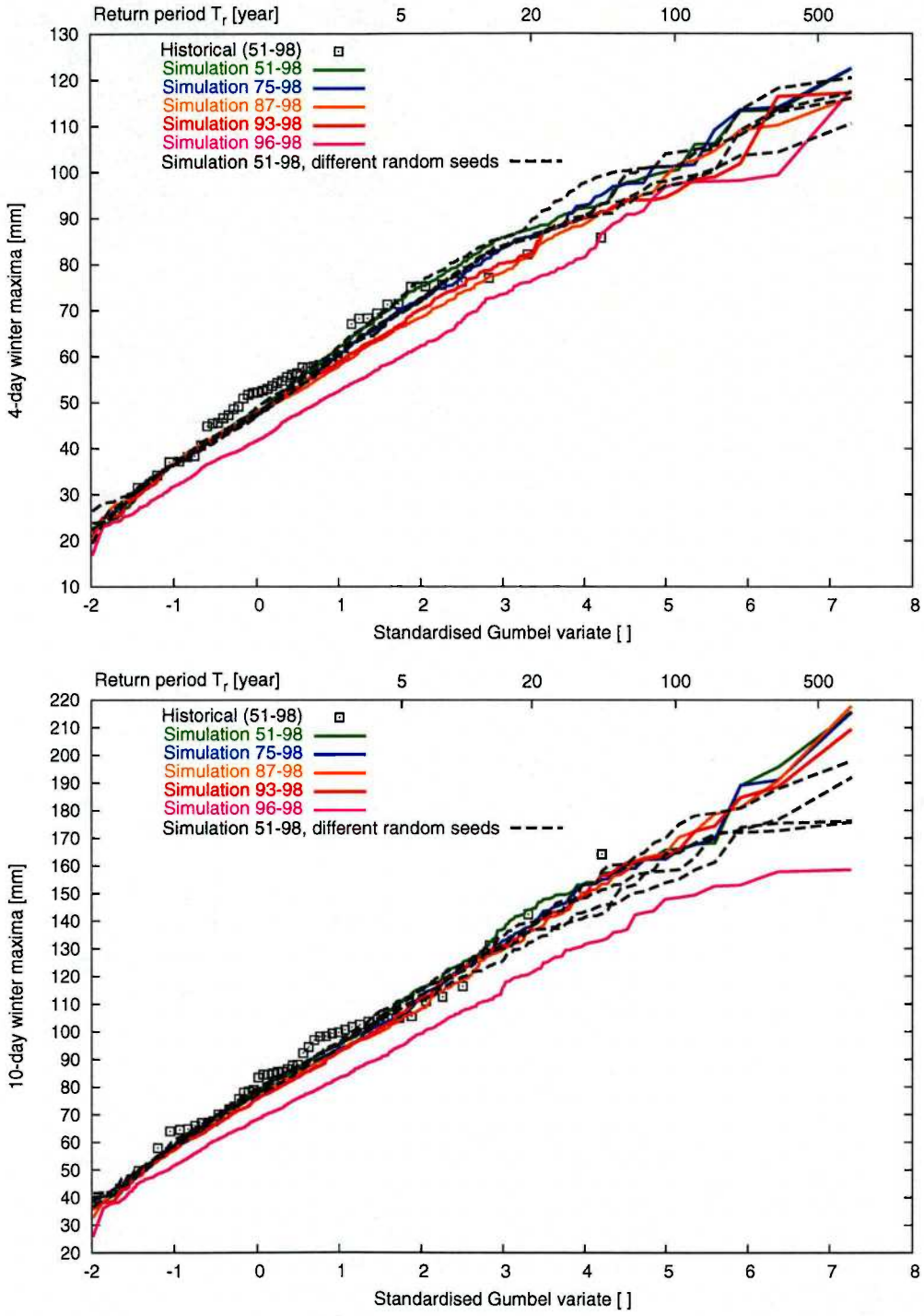

Figure 4.2: Gumbel plots of winter maxima of 4- and 10-day basin-average precipitation for the five simulations 51-98, 75-98, 87-98, 93-98 and 96-98 (solid coloured lines) and the historical data (black squares). The dashed curves represent different simulation runs using sub-catchment data for '51-'98.

5 Simulation of precipitation and temperature for the entire Meuse

In this chapter the resampling methods are applied to simulate long daily sequences of precipitation for all 16 (Belgian and French) sub-catchments of the Meuse upstream of Borgharen, using the methods described in Chapter 3 and 4. The simulations use station temperature and precipitation records as active variables and deliver sub-catchment precipitation data as passive variables. Two different base periods were considered for the simulations:

- **1961-1998**
  Historical precipitation records for all sub-catchments are available for this period. The resampling algorithm presented in Chapter 3 is used. The extra step, introduced in Chapter 4 to substitute missing historical days is not applied in this case.

- **1930-1998 (1940 excluded)**
  The sub-catchment data are only available from 1961 for the French basin and from 1951 for the Belgian basin. Complete sets of sub-catchment precipitation are only available from 1961. Therefore, in the resampling algorithm each historical day sampled from before 1961, must be substituted by a day after 1961, as described in Chapter 4.

For each base period a simulation of 3000 years was performed.

5.1 Simulation based on the period 1961-1998

Seven precipitation records (Rochefort, Stavelot, Uccle, Chiny, Le Chesne, Langres and Neufchâteau) and four daily temperature records (Aachen, Uccle, Langres and Reims) were selected from the stations listed in Table 2.1 as base material for the simulation. These stations were found to be the most representative of the Meuse area, because of their locations and their average annual precipitation amounts. All precipitation and temperature records were first standardised separately using (3.3) for temperature data and (3.4) for precipitation data. The summary statistics used in the feature vector were already defined in Section 3.3.

Means, standard deviations and autocorrelation

To assess the performance of the simulation the monthly means M, monthly standard deviations s_{M} and daily standard deviations s_{D} were calculated from the historical records and the simulated series of areal precipitation P_i (16 sub-catchments) and temperature T_i (4 stations). To avoid the influence of seasonal variation, M, s_{M} and s_{D} were calculated for each month separately, after which the estimates were averaged over the months October to March (for the winter half-year) or April to September (for the summer half-year), yielding the averaged estimates $\overline{M}$, $\overline{s}_{\text{M}}$ and $\overline{s}_{\text{D}}$ for the historical records. The same procedure was followed for the autocorrelation coefficients r_l, resulting in the averaged estimates $\overline{r}_l$ for

each lag l. The reproduction of the means, standard deviations and temporal correlation in the simulated precipitation is crucial to the realistic simulation of multi-day amounts. These in turn are of main interest because of the high river discharges they can induce.

In order to compare the 3000-year simulated series to the historical records, the simulated series were subdivided into 78 runs of 38 years. M, s_{M}, s_{D} and the r_l were obtained for each run separately and the estimates were averaged over the runs, which led to the averaged estimates $\overline{M}^*$, $\overline{s}^*_{\text{M}}$, $\overline{s}^*_{\text{D}}$ and $\overline{r}^*_l$ for the simulations. The differences between the simulated and historical estimates were then averaged over all sub-catchments for the precipitation and all stations for the temperature, i.e.:

$$\Delta\overline{M} = \sum_{i=1}^{N_p,N_t} \lambda_i \left(\overline{M}^* - \overline{M}\right)_i \tag{5.1}$$

for the monthly mean,

$$\Delta\overline{s}_{\text{M}} = \sum_{i=1}^{N_p,N_t} \lambda_i \left(\frac{\overline{s}^*_{\text{M}} - \overline{s}_{\text{M}}}{\overline{s}_{\text{M}}} * 100\%\right)_i \quad \text{and} \quad \Delta\overline{s}_{\text{D}} = \sum_{i=1}^{N_p,N_t} \lambda_i \left(\frac{\overline{s}^*_{\text{D}} - \overline{s}_{\text{D}}}{\overline{s}_{\text{D}}} * 100\%\right)_i \tag{5.2}$$

for the monthly and daily standard deviation and

$$\overline{\Delta r_l} = \sum_{i=1}^{N_p,N_t} \lambda_i \left(r_l^* - \overline{r_l}\right)_i \tag{5.3}$$

for each of the autocorrelation coefficients. The subscript i runs from 1 to $N_p = 16$ for precipitation, or from 1 to $N_t = 4$ for temperature. For precipitation the weight-factor λ_i is proportional to the area of the i-th sub-catchment, such that the sum of the weight-factors equals unity. For temperature the weights are all 1/4. The results are listed in Table 5.1 for the winter half-year and in Table 5.2 for the summer half-year.

The biases for precipitation are generally small. For both winter and summer the bias in the monthly standard deviations is smaller than found in the simulations for the Rhine basin (Beersma, 2002) as a result of the inclusion of a 4-day memory into the feature vector. The bias of the monthly standard deviation is larger in summer than in winter, but still within the double standard error of the historical estimate. There is a small, but significant bias in the first-order autocorrelation coefficient r_1 for both summer and winter. This bias is comparable with that for the simulations for the Rhine basin (Beersma, 2002).

For the temperature the biases in r_1 are even more apparent and there is also a significant bias in r_2 for some of the stations. Figure 5.1 compares the autocorrelation coefficients for winter and summer for both the precipitation and the temperature. This figure clearly shows that the autocorrelation of precipitation is weaker than that of temperature and that the coefficients for summer are smaller than the corresponding coefficients for winter both for precipitation and temperature. The third- to fifth-order autocorrelation coefficients of the temperature tend to be overestimated by the simulation in winter as well as in summer. The autocorrelation of temperature is less important for the Meuse basin than the autocorrelation of precipitation.

Table 5.1: Performance of the 3000-year simulation based on the period 1961-1998 for the winter half-year (October-March). For the montly mean and standard deviation (M and s_M), the daily standard deviation (s_D) and the first- and second-order autocorrelation coefficient (r_1 and r_2) the systematic difference between simulated and historical records is shown, followed by twice the standard error se of the historical estimate. The results are given for the areal precipitation of the sub-catchments in the upper table and for the station temperatures in the lower table. The bottom lines represent the statistics of the basin-averaged series for precipitation and the station-averaged series for temperature. Significant biases are printed in bold.

Precipitation

$\Delta\overline{M}$ (mm)	2×se (mm)	$\Delta\overline{s}_M$ (%)	2×se (%)	$\Delta\overline{s}_D$ (%)	2×se (%)	$\Delta\overline{r}_1$	2×se	$\Delta\overline{r}_2$	2×se	Area (km^2)	
-2.7	6.3	-1.8	10.9	-0.4	6.0	-0.017	0.033	0.004	0.031	2575	1
-3.0	6.3	-0.9	11.5	-0.6	5.8	-0.020	0.036	-0.003	0.029	1283	2
-3.0	6.1	-0.6	11.6	-0.7	5.9	-0.027	0.032	-0.013	0.027	2192	3
-3.1	6.0	-1.4	11.9	-0.8	5.4	-0.030	0.031	-0.022	0.031	2241	4
-1.7	7.7	2.4	10.7	3.0	5.8	**-0.043**	0.027	-0.024	0.026	1213	5
-2.0	6.0	-0.9	10.4	2.2	5.6	**-0.045**	0.030	-0.026	0.027	525	6
-2.3	5.4	1.3	9.6	1.6	5.0	-0.020	0.026	-0.011	0.025	1109	7
-1.7	5.5	3.7	10.6	2.3	5.5	-0.011	0.028	-0.007	0.022	1302	8
-1.9	4.9	0.4	9.3	1.2	5.3	-0.025	0.026	-0.004	0.026	1679	9B
-3.1	5.1	-3.3	12.0	-1.4	5.6	**-0.037**	0.033	-0.018	0.033	1055	9F
-2.1	4.2	2.6	8.4	-0.1	5.3	-0.008	0.027	0.001	0.025	1546	10
-1.9	4.3	2.6	7.8	-0.2	5.4	-0.011	0.027	0.001	0.025	344	11
-2.6	5.4	3.4	9.4	0.8	5.1	-0.006	0.029	-0.004	0.024	1588	12
-2.9	6.4	1.5	8.5	0.1	5.6	-0.018	0.027	-0.014	0.025	1044	13
-2.7	5.8	2.0	7.8	0.0	5.3	**-0.029**	0.026	-0.015	0.025	680	14
-1.5	4.1	5.6	7.8	0.3	6.4	-0.012	0.030	0.007	0.027	455	15
-2.5	4.3	0.5	10.8	0.3	4.9	**-0.022**	0.017	-0.009	0.022	20831	Basin

Temperature

$\Delta\overline{M}$ (°C)	2×se	$\Delta\overline{s}_M$ (%)	2×se	$\Delta\overline{s}_D$ (%)	2×se	$\Delta\overline{r}_1$	2×se	$\Delta\overline{r}_2$	2×se	Station
0.0	0.3	-6.7	12.0	-2.1	4.6	**-0.080**	0.014	-0.023	0.028	Aachen
0.0	0.3	-4.3	11.2	-2.5	4.5	**-0.057**	0.013	-0.019	0.026	Langres
0.0	0.3	-0.3	12.3	-1.9	4.8	**-0.027**	0.014	**0.031**	0.028	Reims
0.0	0.3	-4.9	12.5	-2.3	4.9	**-0.035**	0.012	0.003	0.026	Uccle
0.0	0.3	-4.0	11.8	-2.0	4.9	**-0.035**	0.012	0.003	0.026	Station avg.

Multi-day extremes

For each winter and summer season the maximum 4-,10- and 30-day amounts were determined. These multi-day maxima were calculated from the basin-average daily precipitation (area-weighted average over the sub-catchments). Only those multi-day periods were considered that were entirely within the season of interest. Figure 5.2 compares the Gumbel plots of the multi-day winter maxima of the simulation (solid line) and the historical series (squares). There are 37 winter maxima in the historical record, corresponding to 37 winter seasons in 38 years. To get an impression of the uncertainty of the simulated extremes,

Table 5.2: Same as Table 5.1, but now for the summer half-year (April-September).

Precipitation

$\Delta\overline{M}$ (mm)	2×*se*	$\Delta\overline{s}_M$ (%)	2×*se*	$\Delta\overline{s}_D$ (%)	2×*se*	$\Delta\overline{r}_1$	2×*se*	$\Delta\overline{r}_2$	2×*se*	Area (km^2)	
-1.7	4.2	-11.2	14.2	-1.3	5.2	-0.039	0.043	-0.025	0.041	2575	1
-1.8	4.2	-7.2	10.8	-0.9	4.8	**-0.035**	0.034	-0.009	0.034	1283	2
-1.8	4.3	-6.0	10.2	-0.7	4.5	**-0.035**	0.031	-0.002	0.031	2192	3
-2.0	4.1	-4.6	9.0	-0.9	3.7	-0.023	0.033	-0.001	0.034	2241	4
-3.5	4.8	-3.7	8.0	-0.7	3.5	**-0.026**	0.026	-0.001	0.025	1213	5
-2.5	4.0	-1.5	9.0	-0.4	4.3	**-0.038**	0.031	0.009	0.029	525	6
-2.7	4.1	-0.9	8.4	-0.3	5.5	-0.024	0.037	0.009	0.030	1109	7
-2.9	4.0	-0.1	8.2	-0.1	3.5	-0.013	0.027	0.003	0.026	1302	8
-2.3	3.8	-3.2	11.2	-0.2	5.9	-0.038	0.041	0.011	0.024	1679	9B
-1.7	4.1	-7.2	10.3	-0.9	5.2	**-0.053**	0.029	0.000	0.030	1055	9F
-3.4	3.6	-1.8	11.0	-1.0	4.9	-0.025	0.028	-0.005	0.030	1546	10
-2.2	3.6	-0.8	10.4	1.4	5.1	**-0.027**	0.025	0.007	0.025	344	11
-3.6	4.1	2.4	8.6	-0.8	4.5	-0.007	0.026	0.006	0.027	1588	12
-4.5	4.7	-1.2	11.0	-1.9	4.5	-0.010	0.031	0.008	0.031	1044	13
-4.5	4.9	-1.1	11.4	-0.9	4.6	-0.030	0.031	-0.001	0.032	680	14
-2.5	3.8	-0.8	11.4	2.1	6.3	**-0.041**	0.031	-0.002	0.028	455	15
-2.6	3.0	-4.0	9.3	-0.7	3.6	**-0.029**	0.019	-0.002	0.021	20831	Basin

Temperature

$\Delta\overline{M}$ (°C)	2×*se*	$\Delta\overline{s}_M$ (%)	2×*se*	$\Delta\overline{s}_D$ (%)	2×*se*	$\Delta\overline{r}_1$	2×*se*	$\Delta\overline{r}_2$	2×*se*	Station
0.1	0.2	4.5	8.6	1.3	2.8	**-0.051**	0.017	0.013	0.028	Aachen
0.2	0.3	4.4	8.7	0.9	2.3	**-0.032**	0.013	**0.026**	0.024	Langres
0.1	0.2	6.3	10.9	1.4	3.1	**-0.017**	0.014	**0.042**	0.029	Reims
0.1	0.2	4.6	9.0	1.7	3.1	**-0.029**	0.015	0.014	0.027	Uccle
0.1	0.4	4.9	8.4	1.3	4.0	**-0.032**	0.013	**0.024**	0.019	Station avg.

the 3000-year simulation was broken up into 78 segments of 38 years, which were assumed to be independend members of an ensemble. For each segment an ordered list of winter extremes was calculated. The 90%-envelope (dashed curves) in Figure 5.2 represents the values which are exceeded by 5% (upper curve) and 95% (lower curve) of the segments for each return period separately. This gives an indication to what extent the simulated and the historical maxima are systematically different. It should be noted, however, that only 30 to 50% of the 38-year segments are entirely within the 90%-envelope, as indicated in the figure panels.

For the winter season nearly all historical maxima are well within the 90%-intervals for 4-,10- and 30-day totals. For the 30-day amounts the least agreement between simulated and historical maxima is found. A very high maximum of 300 mm is found in December 1993, which is exceeded once in 235 years by the simulation. The 10-day maxima found in December 1993 (which coincides with the aforementioned 30-day event) and January 1995 correspond to the Meuse floods experienced in those years. The maximum of 164 mm in 1995 corresponds to a return period of approximately 170 years in the simulation. Figure

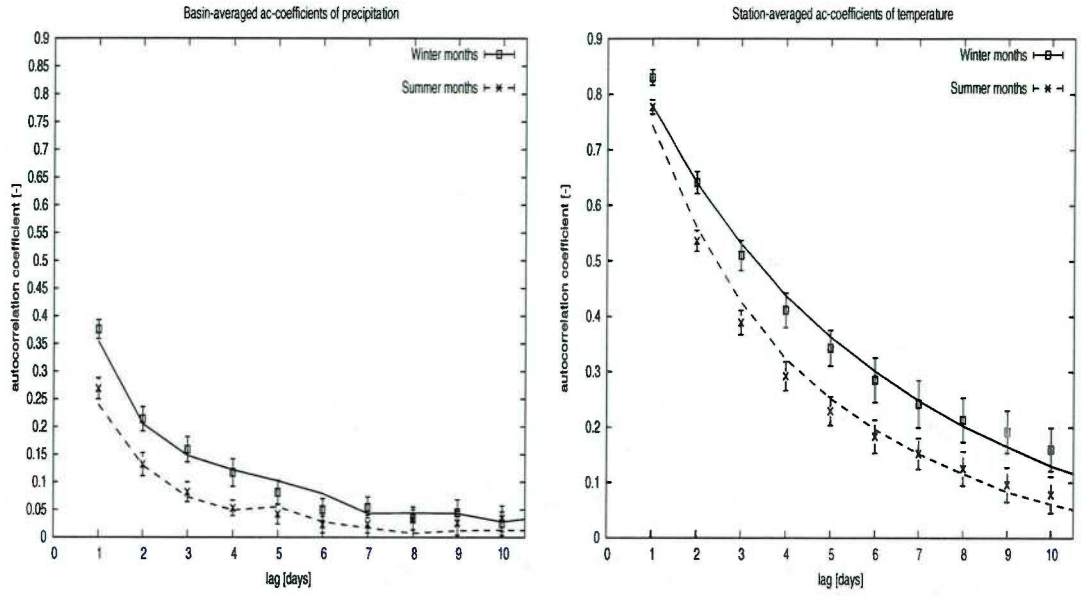

Figure 5.1: Averaged autocorrelation coefficients over the sub-catchments for precipition (left) and over the stations for temperature (right). The error bars represent the $2\times se$ intervals, centred on the historical estimates. The curves refer to the simulation based on the period 1961-1998. Solid curves (and boxes) correspond to the winter months (October to March), whereas the dashed curves (and '×') correspond to the summer months (April to September).

5.4 shows the daily amounts of areal average precipitation for the French and the Belgian part of the basin in December 1993 and early January 1994. The large amount (30.4 mm) on December 19 in the French part induced a flood wave, which coincided with the peak (38.0 mm) on December 20 in Belgium. This coincidence might have caused that the discharge at Borgharen was higher than could be expected from the basin-average precipitation. The extreme 30-day amount was measured between December 7 and January 5. An analysis of this event is given by van Meijgaard (1993).

Figure 5.3 shows Gumbel plots for the summer season. The ordered maxima in summer are lower than those in winter, though the intensity of individual showers is higher. This can be explained by the fact that in summer spatial and temporal correlation of rainfall is generally lower than in winter. For all three durations the distribution of the historical maxima is well reproduced by the simulation. A notable point, however, is that the exceptionally large 30-day amount in July 1980 (244 mm) exceeds the largest 30-day amount in the 3000-year simulation (239 mm). Figure 5.5 shows the basin-average daily amounts for this event and the second largest 30-day summer event in July 1966. In this figure, the temporal pattern of the 1980 event does not appear to be exceptional. Nevertheless, the 30-day maximum of 1980 exceeds that of 1966 by more than 60 mm.

Additional runs for the period 1961-1998 were conducted using the full set of rainfall stations listed in Table 2.1 to test the effect of relatively dry stations (St. Quentin, Reims, Vouziers and Nancy) on the generated rainfall series. The results were similar to those based on the chosen subset of stations.

Furthermore, 3000-year simulations have been performed in which the number of days in the memory element of the feature vector was set to 30 or 60 days. This was done to

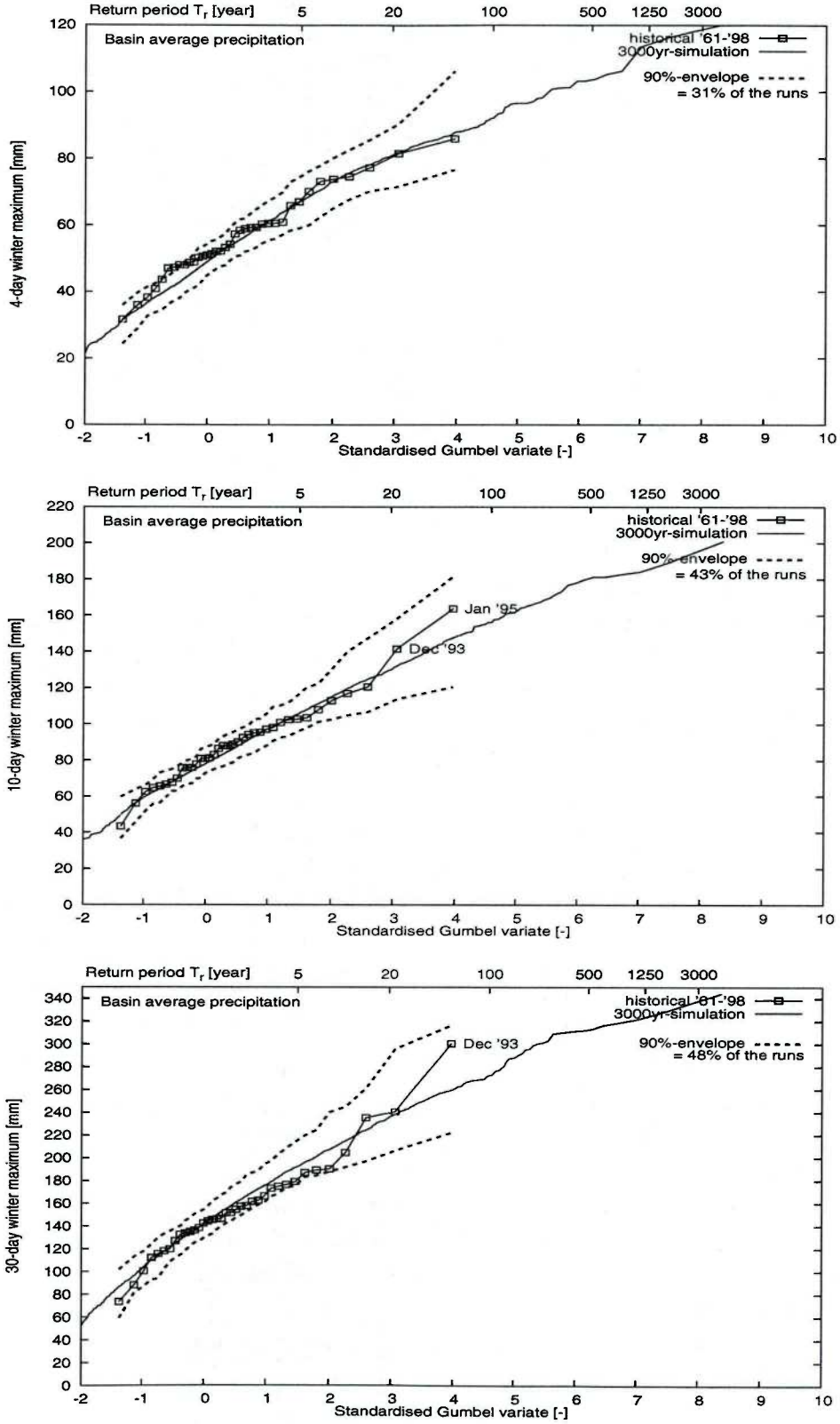

Figure 5.2: Gumbel plots of the 4-, 10- and 30-day winter maxima (basin-average precipitation). The maxima in the historical record (37 seasons) are shown as squares. The solid curve represents the 3000-year simulation based on the period 1961-1998 and the dashed curves show the 90%-envelope of 38-year sections of the simulation. In each panel the percentage of 38-year sections is given, whose Gumbel plot lies entirely within the 90%-envelope. For each return period this interval is representative of the variability of the 37 sorted historical maxima and *not* of the maxima in the 3000-year simulation.

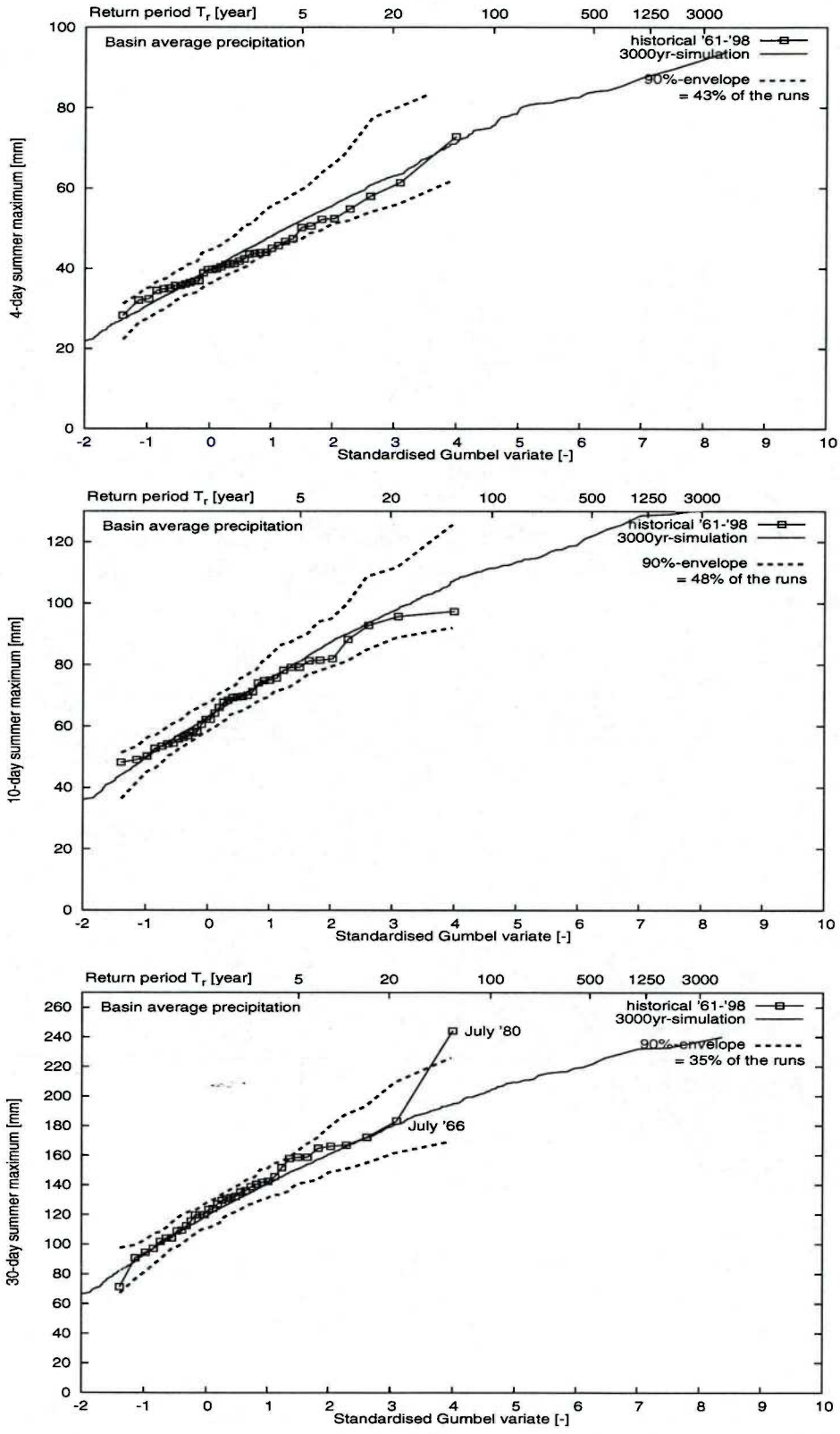

Figure 5.3: Same as Figure 5.2, but now for the summer maxima in the historical record (38 seasons) and the 3000-year simulation.

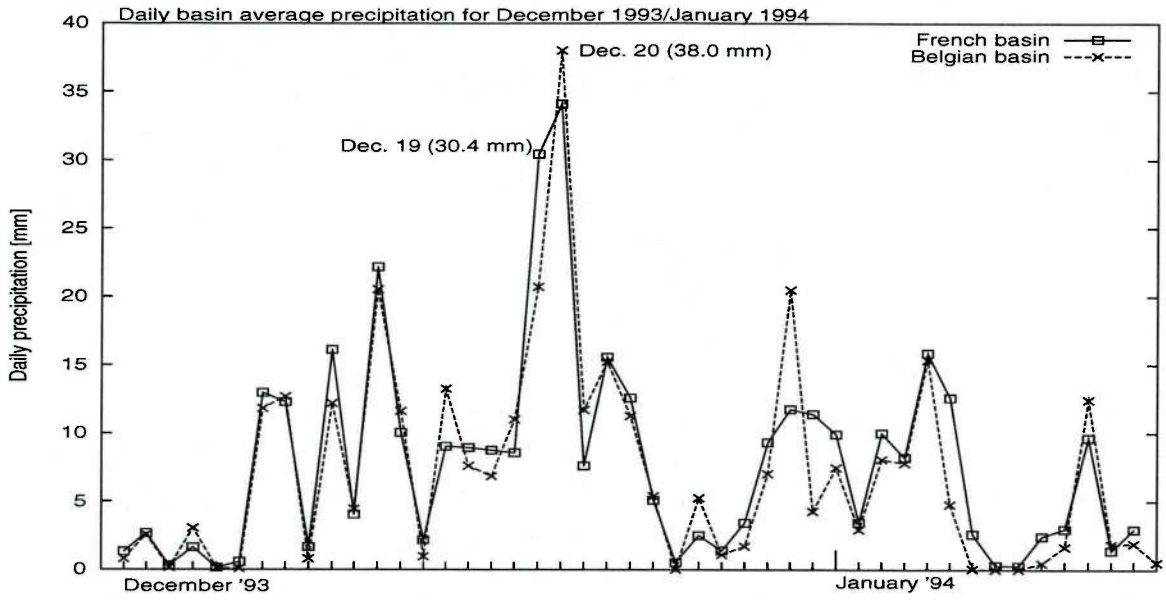

Figure 5.4: Daily basin-average precipitation for December 1993 and the first days of January 1994 for the French basin (sub-catchments 1 to 4 and 9F) and the Belgian basin (remaining sub-catchments).

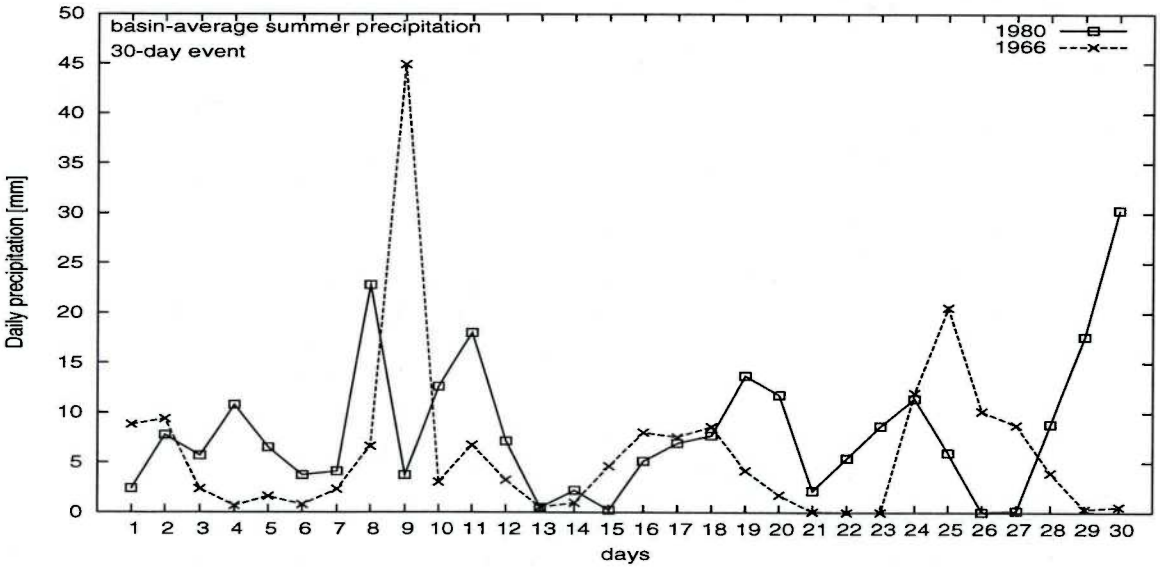

Figure 5.5: Daily basin-average precipitation for the 30-day event ending on July 20, 1980 (244 mm) and the 30-day event ending on July 9, 1966 (183 mm).

investigate the effect on the occurrence of exceptional 30-day rainfall events in winter, such as the December '93 event. Also simulations with both a 4-day and a 30-day memory element were done (also with a length of 3000 year). However, none of those simulations seemed to influence the frequency of exceptional multi-day amounts in winter.

Table 5.3: The upper quintile means (QM5) in mm of the simulated 4-,10- and 30-day maxima in summer and winter for both base periods. The last two columns present the percentage difference between the simulations based on '61-'98 and '30-'98.

	base period '30-'98		base period '61-'98		difference (%)	
	winter	summer	winter	summer	winter	summer
4-day	74.0	58.4	77.4	59.9	4.6	2.6
10-day	118.2	90.6	124.9	92.3	5.7	1.9
30-day	214.0	167.3	226.0	169.9	5.6	1.6

5.2 Simulation based on the period 1930-1998

For the period 1930-1998 (excluding 1940), the same stations were used as in Chapter 4. The modified resampling algorithm discussed in that chapter makes it possible to combine these records with the shorter records of sub-catchment precipitation for the period 1961-1998. For historical days sampled from before 1961 the best substitute day is sought in the period 1961-1998. The (standardised) sub-catchment data for this substitute day are then delivered as the data for the considered simulated day. The resulting series contains the individual daily values of area-average precipitation from the shorter period, but it has the same statistical properties as the area-average precipitation for the longer period on which the resampling of station data is based.

Table 5.3 shows the upper quintile means (QM5) of the 4-, 10- and 30-day maxima in winter and summer for the simulation based on 1930-1998 and the simulation based on 1961-1998 (discussed in Section 5.1). QM5 is defined as the average of the upper 20% of the values and generally corresponds to a return period of about 13 years. The QM5 values for the simulated winter maxima based on 1961-1998 are about 5% higher than those based on 1930-1998. For the summer maxima the differences between the QM5 values of the two simulations are smaller.

Figure 5.6 compares the Gumbel plots of the 4-,10- and 30-day winter maxima for the simulation based on the period 1961-1998 to those based on 1930-1998. The difference between the simulations is most obvious for return periods between 5 and 20 years. For longer return periods the uncertainty increases considerably and the systematic difference between the simulations becomes less clear. The observed differences between the simulated winter maxima in Table 5.3 and Figure 5.6 are in line with the difference of 3.5% between the mean winter amounts for the two periods (Section 2.1).

In Figure 5.7 the highest simulated 4-day and 10-day winter maxima have been plotted against the calendar day on which the multi-day period ended. The encircled events are listed in Table 5.4, together with the two largest historical events. Besides the month and year of occurrence and the 4-day or 10-day amount also the total of the antecedent 30-day period is given. The antecedent situation has a large influence on how the basin reacts to large precipitation amounts. In a wet situation the capacity of the soil to absorb water will be smaller and the discharge reacts stronger to heavy rainfall. The antecedent condition is very dry for the historical December 1986 event and very wet for the historical December 1993 and January 1995 events. The simulated events `Sim2b` and `Sim3b` have even a larger antecedent 30-day rainfall than these historical events.

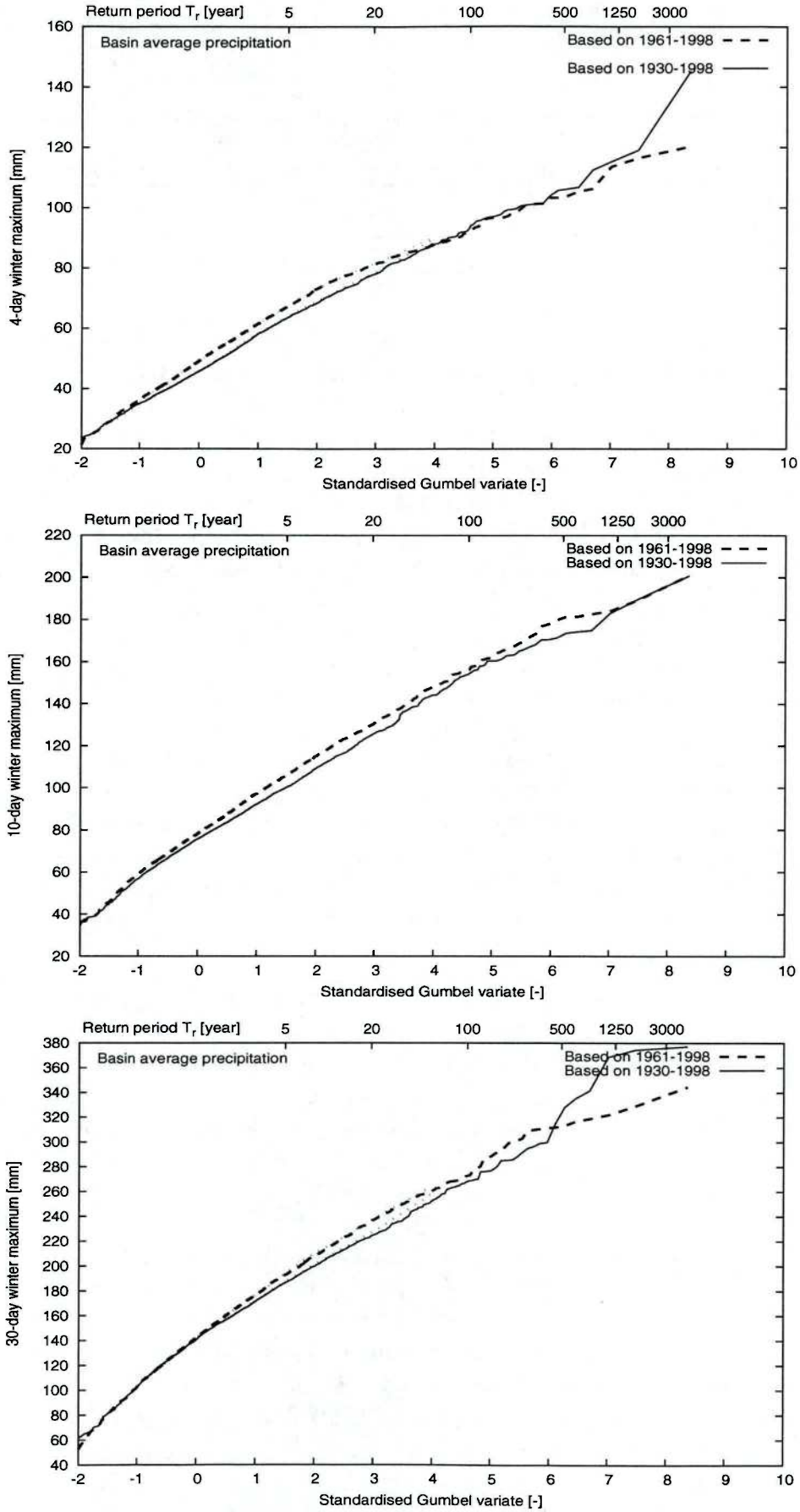

Figure 5.6: Comparison between the ordered winter maxima in 3000-year simulations based on station data from the periods 1961-1998 (dashed) and 1930-1998 (solid). From top to bottom the 4-,10- and 30-day winter maxima are shown.

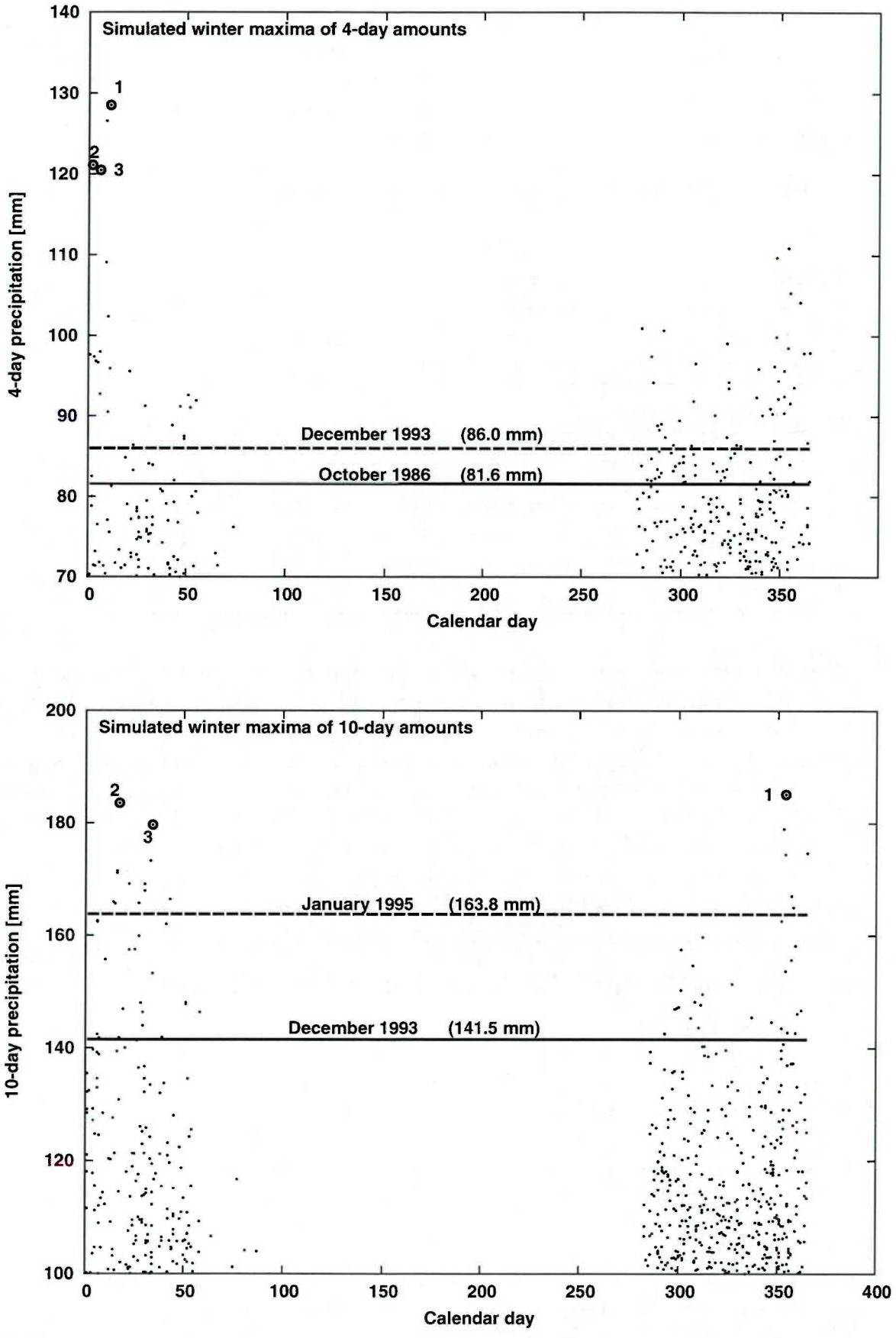

Figure 5.7: The highest winter maxima of 4-day (top) and 10-day (bottom) basin-average precipitation from the 3000-year simulation based on the years 1930-1998. The two horizontal lines show the two largest maxima in the historical record (1961-1998) for both durations.

Table 5.4: Three simulated (base period 1930-1998) and two historical events of extreme 4-day (top) and 10-day (bottom) basin-average precipitation. Events beginning with `His..` refer to the historical data, events beginning with `Sim..` are simulated. The simulated events are encircled in Figure 5.7. P_4 and P_{10} denote the extreme precipitation amounts and P_A the precipitation amount in the antecedent 30-day period.

4-day winter maxima

	Month	Year	P_4 (mm)	P_A (mm)
His1a	December	1993	86.0	127.9
His2a	October	1986	81.6	7.2
Sim1a	January	662	128.5	73.5
Sim2a	January	2135	121.1	61.6
Sim3a	January	847	120.5	125.2

10-day winter maxima

	Month	Year	P_{10} (mm)	P_A (mm)
His1b	January	1995	163.8	139.7
His2b	December	1993	141.5	83.7
Sim1b	December	104	185.1	67.2
Sim2b	January	2587	183.5	217.3
Sim3b	January	2925	179.7	155.5

For the selected simulated 4-day and 10-day precipitation events the daily basin-average amounts and the historical days they were sampled from are listed in Table 5.5. It appears that the high multi-day rainfall amounts of these events are caused by the repetitive occurrence of historical days with large daily precipitation amounts. Repeatedly resampling of the same day within short periods can give rise to very large artificial multi-day events and should therefore be avoided. New simulations show that this repetition is strongly reduced if a moving window of 121 days is used instead of 61 days. This reduction is accompanied by a decrease of approximately 15 mm in the average of the three highest 4-day amounts. For the 10-day amounts, on the other hand, the difference is negligible.

5.3 Simulation of temperatures for additional stations in the basin

From 7 more stations in and around the Meuse basin shorter homogeneous temperature records were available, which were also used in the calibration of the hydrological model. These are Beek, Chimay, Dourbes, Ernage, Forges, Lacuisine and St. Hubert. Except for Beek, which is in the Netherlands, all stations are located in Belgium.

The temperatures of these 7 stations, together with the 4 stations mentioned in Section 2.3, were simulated in the same way as the precipitation for the sub-catchments, using only data from the years 1967-1998. This is the longest period that all 11 temperature records have in common. Historical days before 1967 selected in the simulation were replaced by analogous days between 1967 and 1998, as described in Chapter 4. Although this substitution is not necessary for stations with long records (the stations contributing to the feature vector's temperature element), it was preferable that for each simulated day all temperature values

Table 5.5: Daily values of basin-average precipitation in the selected simulated extreme 4-day (top) and 10-day (bottom) events and the historical days from which they were sampled.

4-day winter maxima

	Sim1a			Sim2a			Sim3a		
Day	hist. day	P		hist. day	P		hist. day	P	
1	93.01.11	41.6	mm	65.12.25	9.9	mm	94.01.12	11.5	mm
2	95.01.22	35.9		93.01.11	42.2		93.01.11	42.0	
3	95.01.22	35.8		94.12.27	33.8		94.12.27	33.8	
4	95.01.26	15.3		93.12.20	35.3		94.12.27	35.2	
Total		128.5			121.1			120.5	

10-day winter maxima

	Sim1b			Sim2b			Sim3b		
Day	hist. day	P		hist. day	P		hist. day	P	
1	95.12.21	14.8	mm	95.01.22	36.0	mm	84.02.06	33.5	mm
2	94.12.27	34.8		95.01.22	35.9		84.02.07	10.0	
3	94.12.27	34.8		80.12.25	2.2		84.02.08	12.5	
4	91.12.22	3.9		95.01.24	14.0		84.02.08	12.5	
5	66.12.12	20.7		95.01.27	19.6		95.01.25	26.3	
6	79.12.14	13.1		95.01.27	19.5		95.01.27	18.3	
7	94.12.16	2.5		95.01.27	19.4		95.01.27	18.2	
8	66.12.12	20.7		84.01.17	3.1		84.02.08	12.3	
9	91.12.20	7.9		81.01.19	6.2		95.01.27	18.1	
10	91.12.21	31.9		95.01.25	27.6		95.01.27	18.1	
Total		185.1			183.5			179.7	

correspond to the same historical day to preserve the spatial correlation of the temperature in the simulations. The substituted temperature was further adjusted using the temperature of the station Uccle as a reference:

$$T_{station}(t_1) = T_{station}(t_2) + [T_{uccle}(t_1) - T_{uccle}(t_2)] \ , \tag{5.4}$$

where t_1 denotes the historical day to be replaced and t_2 is the nearest-neighbour substitute. The Uccle temperature record covers the entire period 1930-1998.

6 Comparison of simulations for the Ourthe catchment

RIZA (Aalders and De Wit, 2004) has conducted hydrological simulations of the Ourthe catchment, using a 1000-year simulation of catchment-average precipitation data described in Wójcik and Buishand (2001). A comparison has been made between this simulation (denoted as Wójcik's simulation) and a 1000-year segment of the currently conducted simulations based on the period 1961-1998 (denoted as Mem). Furthermore, a third 1000-year simulation (NoMem) was considered, which was similar to Mem except that no 4-day memory was used in the feature vector. This was done to assess the effect of the additional memory in the simulations.

Table 6.1 shows the bias of the first- and second-order statistics for the considered simulations. The bias is determined by comparison with the historical daily precipitation for the Ourthe catchment for the period 1961-1998. The biases in the monthly and daily standard deviation are considerably smaller in the current simulations (Mem and NoMem) than in Wójcik's simulation. The biases in the monthly mean are all of the same order. The autocorrelation coefficients are better reproduced in the current simulation than in Wójcik's simulation. The standard deviation of the monthly values is better reproduced by the Mem simulation than by the NoMem simulation as a result of a better reproduction of the higher-order autocorrelation coefficients. However the bias in the monthly mean and the first-order autocorrelation $\overline{r}_1$ slightly increases.

Figure 6.1 compares the 4-, 10- and 30-day winter maxima for the three considered simulations. The Mem simulation leads to slightly higher maxima than Wójcik's simulation, in particular for the longer return periods. This is most obvious for the 30-day maxima, where the curve for Wójcik's simulation flattens at 300 mm. The curves for the NoMem simulation are comparable to those of Wójcik's simulation for all durations, except that the two highest 10-day amounts in the NoMem simulation are higher.

The shown results indicate that the differences between the current simulations and Wójcik's simulation can partly be ascribed to the inclusion of the memory. The effect of the memory is in particular visible in the second- to fourth-order autocorrelation coefficient and in the

Table 6.1: Biases of the first- and second-order statistics for the currently performed simulations (with base period '61-'98) and Wójcik's 1000-year simulation for the Ourthe catchment. The bias in the monthly mean $\overline{M}$ and standard deviation $\overline{s}_{\mathrm{M}}$, the daily standard deviation $\overline{s}_{\mathrm{D}}$ and the autocorrelation coefficients $\overline{r}_1$ to $\overline{r}_4$ for the winter half-year (October-March) are shown. The bottom line gives the double standard error of the historical estimate.

	$\Delta\overline{M}$		$\Delta\overline{s}_{\mathrm{M}}$		$\Delta\overline{s}_{\mathrm{D}}$		$\Delta\overline{r}_1$	$\Delta\overline{r}_2$	$\Delta\overline{r}_3$	$\Delta\overline{r}_4$
Mem	-2.5	mm	1.6	%	0.2	%	-0.006	-0.002	0.000	0.009
NoMem	-1.7		-3.5		0.5		0.003	-0.009	-0.018	-0.021
Wójcik	-2.7		-9.1		-3.5		-0.008	-0.015	0.025	0.025
$2 \times se$	5.4		9.4		5.1		0.029	0.024	0.030	0.033

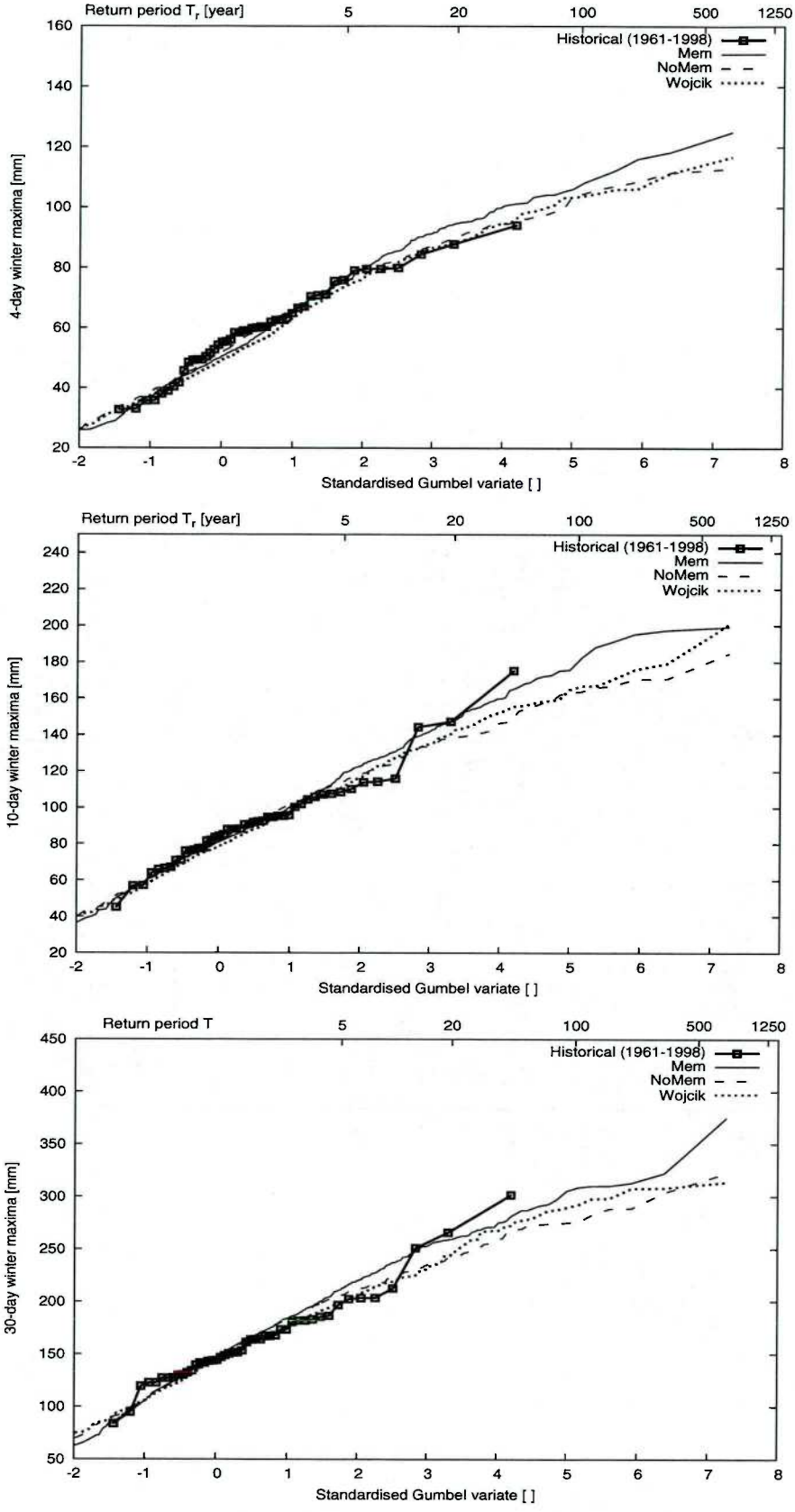

Figure 6.1: Comparison between the multi-day winter maxima for the Ourthe catchment from the Mem and Nomem simulation and Wójcik's simulation. All three simulations have a length of 1000 year. From top to bottom the 4-day, 10-day and 30-day winter maxima are shown.

multi-day winter maxima. The choice of the stations used in the feature vector and random fluctuations also partially account for the differences between the simulations.

7 Conclusions

In this report the principle of nearest-neighbour resampling was applied to a set of precipitation and temperature stations in the Meuse basin. The precipitation of 16 sub-catchments of the river Meuse and the temperature of 11 stations were simulated passively. For these variables the areal rainfall records from 1961-1998 and the temperature records from 1967-1998 are used. A modified resampling algorithm was required for the passive simulation of variables with historical records shorter than the base period of the simulation. This algorithm involved a secondary nearest-neighbour step.

A 3000-year simulation based on station records for the period 1961-1998 has been performed. For precipitation no significant bias was found in the simulated monthly mean and standard deviation, the daily standard deviation and the autocorrelation coefficients of second order and higher. There was a small, but significant, underestimation of the first-order autocorrelation coefficient. This was also found in earlier simulations with the nearest-neighbour method.

There is a good agreement between the simulated and historical quantiles of the 4-,10- and 30-day seasonal maxima of area-average precipitation. In nearly all cases the Gumbel plot for the historical area-averages lies within the 90%-envelope of the simulated data. However, the historical records contain three rare multi-day events, which occur less frequently in the simulated data than would be expected. These events took place in July 1980, December 1993 and January 1995 and are well-known in the history of extreme river discharges of the Meuse. The 30-day maximum amount in June/July 1980 is not exceeded in the 3000-year simulation, indicating a failure of the resampling model to generate very excessive 30-day summer precipitation.

The bias in the simulated temperature has been calculated for the stations Aachen, Langres, Reims and Uccle. No significant bias was found in either the simulated monthly mean and standard deviation or in the daily standard deviation. However, the first-order autocorrelation coefficient was significantly underestimated for all stations. A significant positive bias in the second-order autocorrelation coefficient was found for Reims. In a number of cases there was also a significant positive bias in the second-order autocorrelation coefficient.

Also a 3000-year simulation has been performed, which was based on station records for the period 1930-1998 (excluding the year 1940). The upper quintile means of the seasonal maxima of multi-day amounts were lower in this simulation than in the simulation based on the period 1961-1998, in particular for the winter half-year ($\approx$5%).

The currently simulated precipitation for the Ourthe catchment (which is simulated as a part of the Meuse basin) has improved, compared to Wójcik's Ourthe simulation. This can partly be ascribed to the inclusion of a 4-day memory in the feature vector, which affects the higher order autocorrelation.

It was found that in simulations using a window of 61 days the most extreme multi-day amounts were formed by the repetition of certain wet historical days. A broader window of

121 days reduces this repetition. As a result, the most extreme multi-day events are also lower when this window is applied, in particular for the 4-day duration.

Acknowledgements

The station records and sub-catchment data for the Belgian part of the Meuse basin were provided by the Royal Meteorological Institute of Belgium (RMIB). The French station data were made available by Météo France. The work was performed in co-operation with the Institute for Inland Water Management and Waste Water Treatment (RIZA).

References

Aalders, P. and De Wit, M. J. M. (2004). Rainfall Generator for the Meuse basin; Case study Ourthe basin. RIZA werkdocument 2004.137X, RIZA, Arnhem.

Beersma, J. J. (2002). Rainfall generator for the Rhine basin: Description of 1000-year simulations. KNMI-publication 186-V, KNMI, De Bilt.

Bennekom, A. R. V. and Parmet, B. W. A. H. (1998). Bemessungsabfluβ in den niederlanden; menschliche einflüsse und andere unsicherheiten, Bemessungsabfluβ in den Niederlanden; menschliche Einflüsse und andere Unsicherheiten, In *Zukunft der Hydrologie in Deutschland, BfG Mitteilung 16.* Bundesanstalt für Gewässerkunde, Koblenz, 125–131.

Buishand, T. A. and Beersma, J. J. (1993). Jacknife tests for differences in autocorrelation between climate time series. *J. Climate*, 6:2490–2495.

Buishand, T. A. and Beersma, J. J. (1996). Statistical tests for comparison of daily variability in observed and simulated climates. *J. Climate*, 9:2538–2550. (Corrigendum, *J. Climate*, 10:818, 1997).

Buishand, T. A. and Brandsma, T. (1996). Rainfall generator for the Rhine catchment: a feasibility study. Technical Report TR-183, KNMI, De Bilt.

Delft Hydraulics (1994). Onderzoek watersnood Maas. 15 vol., Delft, the Netherlands.

Delft Hydraulics and EAC-RAND (1993). Toetsing uitsgangpunten rivierdijkversterkingen, Deelrapport 2: Maatgevende belastingen. Delft Hydraulics, Emmeloord, and European American center for Policy Analysis (EAC-RAND), Delft, the Netherlands.

Lall, U. and Sharma, A. (1996). A nearest neighbor bootstrap for resampling hydrologic time series. *Water Resour. Res.*, 32:679–693.

Leander, R. and Buishand, T. A. (2004a). Rainfall Generator for the Meuse Basin: Inventory and homogeneity analysis of long daily precipitation records. KNMI-publication 196-II, KNMI, De Bilt.

Leander, R. and Buishand, T. A. (2004b). Estimation of areal precipitation from station records. Memorandum `KA-04-11`, KNMI, De Bilt.

Middelkoop, H. and van Haselen, C. O. G. (1999). Twice a river. Rhine and Meuse in the Netherlands. RIZA report no. 99003, RIZA, Arnhem.

van de Langemheen, W. and Berger, H. E. J. (2001). Hydraulische randvoorwaarden 2001: maatgevende afvoeren Rijn en Maas. RIZA report no. 2002.014, RIZA, Arnhem.

van Deursen, W. (2004). Afregelen HBV model Maasstroomgebied. Report, Carthago Consultancy, Rotterdam.

van Meijgaard, E. (1993). Evaluatie van neerslagprognoses van numerieke modellen voor de Belgische Ardennen in december 1993. Technical Report TR-169, KNMI, De Bilt.

Wójcik, R., Beersma, J. J., and Buishand, T. A. (2000). Rainfall generator for the Rhine basin: Multi-site generation of weather variables for the entire drainage area. KNMI-publication 186-IV, KNMI, De Bilt.

Wójcik, R. and Buishand, T. A. (2001). Rainfall generator for the Meuse basin: Simulation of 6-hourly rainfall and temperature for the Ourthe catchment. KNMI-publication 196-I, KNMI, De Bilt.

Young, K. C. (1994). A multivariate chain model for simulating climatic parameters from daily data. *J. Appl. Meteorol.*, 33:661–671.